Chemical Physics Letters 510 (2011) 202–207

Contents lists available at ScienceDirect

Chemical Physics Letters

journal homepage: www.elsevier.com/locate/cplett

Stokes' shift dynamics in alkylimidazolium aluminate ionic liquids: Domination of solute-IL dipole–dipole interaction

Snehasis Daschakraborty, Ranjit Biswas *

S.N. Bose National Centre for Basic Sciences, JD Block, Sector III, Salt Lake, Kolkata 700 098, India

ARTICLE INFO

Article history:
Received 2 March 2011
In final form 13 May 2011
Available online 17 May 2011

ABSTRACT

A molecular theory is employed to predict the Stokes' shift dynamics for a dipolar solute, C153, in six different alkylimidazolium ionic liquids (ILs) containing a fixed anion, tetra(hexafluoroisopropoxy)aluminate. Calculated shifts in these ILs at ~343 K range ~2300–3700 cm^{-1}, and a dominating contribution (~75–85%) arises from the solute-IL dipole–dipole interaction. Inclusion of solvent-libration predicts ~50% ultrafast component in the total dynamics. Although the predicted dynamics is faster than in other ILs, calculated shifts follow the same linear correlation with ion size-ratio. Furthermore, model calculations explore the solute-IL size-ratio dependence of the interaction contributions to the shift, and investigates the relative importance of solvent rotational and translational modes for IL dynamics.

1. Introduction

Recently, a new class of ionic liquids (ILs) based on alkylimidazolium cations and the weakly coordinating anion, tetra(hexafluoroisopropoxy)aluminate has been synthesised and their important physical properties measured [1]. These ILs are low viscous solvents compared to other ionic liquids [2] and, most interestingly, the change in viscosity upon variation of the alkyl group attached to imidazolium cation is very small (η = 9–12 cP at 343 K). Subsequently, the validity of hydrodynamic relations for these ILs have been verified by carrying out dielectric relaxation (DR) measurements covering a frequency range up to 20 GHz at a temperature (~343 K) well above their respective melting temperatures [3]. These measurements have indicated strongly stretched relaxation dynamics reminiscent of that observed in highly viscous heterogeneous media approaching glass transition [4]. Because of the chemical structures of the cations and the anion (shown in Scheme 1), extended hydrophobic and hydrophilic domains may form and lead to microscopic phase segregation [5,6] in these low viscous ILs. This might be the reason for the observed strongly stretched relaxation dynamics [3].

Apart from the stretched DR dynamics which directly affects solvation energy relaxation of a dissolved laser-excited solute, the static dielectric constant (ε_0) and ion diameter (σ_+ and σ_-) are two important factors which affect the magnitude of the calculated dynamic Stokes' shift [7,8]. Furthermore, if the solvent dipole moment required as input for such calculations is obtained from either the mean spherical approximation (MSA) [9] or the Cavell's equation [10], ions with heavier molecular weight lead to a larger value of effective dipole moment (μ_{eff}) for an ionic liquid. Larger values of ε_0 or the slowest dispersion magnitude ($\Delta\varepsilon$) also lead to larger μ_{eff} and this, in turn, increases the relative contribution from the solute-IL dipole–dipole interaction contribution to the calculated total dynamic Stokes' shift [7,8,11,12]. In contrast, larger ε_0 decreases the solute-IL dipole–ion interaction contribution via decreasing the ion–solute interaction. Larger size of ions can substantially reduce the collective mode (long wavelength) contributions via the excluded volume effect. These factors naturally motivate one to perform calculations for model ILs characterized by larger values of ε_0 (or $\Delta\varepsilon$), μ_{eff}, $\sigma_{+/-}$ (ion diameter) and larger ion molecular weight in order to explore whether solute-IL dipole–dipole interaction indeed dominates the dynamic Stokes' shift in IL where ion–ion interaction govern physicochemical properties of these liquids. This is an interesting scenario as one expects the solute-IL dipole–ion interaction should determine much of the shift and the related dynamics. ILs based on alkylimidazolium cations and weakly coordinating anion, tetra(hexafluoroisopropoxy)aluminate, are such model ionic liquids which contain a large anion (much larger than studied so far [7,8]) and characterized by higher ε_0 values [3] than others [13,14] at comparable temperature.

In this Letter, we report calculated dynamic Stokes' shifts and solvation response functions at 343 K for a dipolar solute probe, C153, dissolved in six different ionic liquids containing a fixed anion, tetra(hexafluoroisopropoxy)aluminate ($[Al(hfip)_4]^-$), and the following cations: 1-ethyl-3-methylimidazolium ($[C2\text{-}mim]^+$), 1-butyl-3-methylimidazolium ($[C4\text{-}mim]^+$), 1-hexyl-3-methylimidazolium ($[C6\text{-}mim]^+$), 1-allyl-3-methylimidazolium ($[allyl\text{-}mim]^+$), 1-ethyl-2,3-dimethylimidazolium ($[C2\text{-}mmim]^+$) and 1-butyl-2,3-dimethylimidazolium ($[C4\text{-}mmim]^+$). Because of variation in the alkyl chain length attached to the imidazolium cation, σ_+ ranges

* Corresponding author.
E-mail address: rbsnbc@gmail.com (R. Biswas).

0009-2614/$ - see front matter © 2011 Elsevier B.V. All rights reserved.
doi:10.1016/j.cplett.2011.05.027

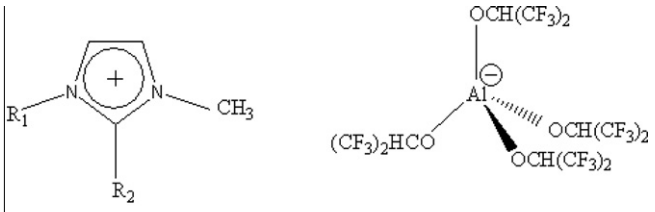

Aluminate ILs studied (R1 = allyl, n-butyl, ethyl, n-hexyl; R2 = H, methyl)

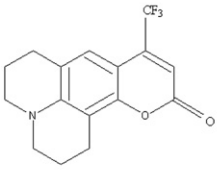

Coumarin 153 (C153)

Scheme 1. Chemical structures of aluminate ILs and the dipolar probe.

[3] between 6.58 and 7.76 Å. σ_-, on the other hand, is 12.5 Å [15], making the ratio between the ion-sizes ($P = \sigma_+/\sigma_-$) vary between ~0.53 and ~0.62. Note that molecular dynamics simulation studies have already suggested substantial effects of ion-size disparity on transport properties in model ILs [16]. In that study, however, cation was considered to be larger than the anion (size held constant) and P was varied between 1 and 5. For the present set of ILs, P obviously falls in the different regime, and the situation is somewhat reverse in the sense that the anion is larger roughly by a factor of 2 than the cations. Interestingly, a systematic study on the effects of P on Stokes' shift dynamics in ILs has not yet been reported. This and the dominating contribution of the dipole–dipole interaction to the total dynamic Stokes' shift constitute the main focus of the present Letter.

2. Theoretical formulation and calculation details

Since the molecular theory used here has already been developed and discussed in detail elsewhere [7,8,11,12,17,18], we only mention the necessary equations along with a brief outline for the calculations. The use of the classical density functional theory [19–21] provides the following expression for the position ($\mathbf{r}$), orientation ($\mathbf{\Omega}$) and time (t) dependent total fluctuating solvation energy for a mobile dipolar solute with distribution function $\rho_s(\mathbf{r}, \mathbf{\Omega}; t)$

$$\Delta E_{\text{total}}(\mathbf{r}, \mathbf{\Omega}; t) = -k_B T \rho_s(\mathbf{r}, \mathbf{\Omega}; t)\left[\int d\mathbf{r}' d\mathbf{\Omega}' c_{sd}(\mathbf{r}, \mathbf{\Omega}; \mathbf{r}', \mathbf{\Omega}')\delta\rho_d(\mathbf{r}', \mathbf{\Omega}'; t) + \sum_{\alpha=1}^{2}\int d\mathbf{r}' c_{s\alpha}(\mathbf{r}, \mathbf{\Omega}; \mathbf{r}')\delta n_\alpha(\mathbf{r}'; t)\right] = \Delta E_{sd}(r, \Omega; t) + \Delta E_{si}(r, \Omega; t) \quad (1)$$

$c_{sd}(\mathbf{r}, \mathbf{\Omega}; \mathbf{r}', \mathbf{\Omega}')$ and $c_{s\alpha}(\mathbf{r}, \mathbf{\Omega}; \mathbf{r}')$ are respectively the position and orientation dependent solute dipole–solvent dipole (dipole–dipole) and solute dipole–ion (dipole–ion) direct correlation functions and α denotes the type of ions (cation and anion). The fluctuations in dipolar density ($\delta\rho_d$) and ion density (δn_α) from the respective bulk values are: $\delta\rho_d(\mathbf{r}, \mathbf{\Omega}) = \rho_d(\mathbf{r}, \mathbf{\Omega}) - \rho_d^0/4\pi$ and $\delta n_\alpha(\mathbf{r}) = n_\alpha(\mathbf{r}) - n_\alpha^0$. The solvation energy–energy correlation function averaged over space ($\mathbf{r}$) and orientation ($\mathbf{\Omega}$) is then written as

$$C_E(t) = C_{sd}(t) + C_{si}(t), \quad (2)$$

where the dipole–dipole interaction contribution given as

$$C_{sd}(t) = \langle \Delta E_{sd}(t)\Delta E_{sd}(0)\rangle = 2\rho_d^0\left(\frac{k_B T}{2\pi}\right)^2\left[\int_0^\infty dk k^2 S^{10}_{\text{solute}}(k;t)|c^{10}_{sd}(k)|^2 S^{10}_{\text{solvent}}(k;t) + 2\int_0^\infty dk k^2 S^{11}_{\text{solute}}(k;t)|c^{11}_{sd}(k)|^2 S^{11}_{\text{solvent}}(k,t)\right], \quad (3)$$

and the dipole–ion interaction term as

$$C_{si}(t) = \langle \Delta E_{si}(t)\Delta E_{si}(0)\rangle = 2\left(\frac{k_B T}{2\pi}\right)^2 \sum_{\alpha,\beta}\sqrt{n_\alpha^0 n_\beta^0} \times \int_0^\infty dk k^2 S^{10}_{\text{solute}}(k;t) c^{10}_{s\alpha}(k) c^{10}_{s\beta}(-k) S^{\text{ion}}_{\alpha\beta}(k,t), \quad (4)$$

Note in writing Eq. (2) the cross-correlation between fluctuating energies has been assumed to vanish due to separation of time-scales involved in fluctuations of dipolar solvent and ion densities. $c^{lm}_{sd}(k)$ represents the wave-number (k) dependent (l, m) component of the static correlation function between the solute and dipolar ion, and $S^{lm}_{\text{solvent}}(k,t)$ is the same component of the orientational dynamic structure factor of the dipolar species. While $c^{lm}_{sd}(k)$ has been obtained from the MSA, $S^{lm}_{\text{solvent}}(k,t)$ has been calculated, as before [7,8,11,12], by using the experimentally measured [3] frequency dependent dielectric function, $\varepsilon(z)$, summarized in Table S1 (Supporting information). The solute self-dynamic structure factor, $S^{lm}_{solute}(k,t)$, has been approximated by its diffusive limit where the rotational and translational diffusion coefficients for a spherical solute with a volume of C153 have been obtained from the IL viscosity using the stick boundary condition.

The longitudinal component of the wave-number dependent direct correlation function between the dipolar solute and ions, $c^{10}_{s\alpha}(k)$, is taken as [7,8],

$$c^{10}_{s\alpha}(k) = -\sqrt{\frac{4\pi}{3}}\left(\frac{4\pi i \mu_1 q_\alpha}{k_B T \varepsilon_0 k}\right)\frac{\sin(kr_c)}{kr_c} = -\sqrt{\frac{4\pi}{3}}\left(\frac{4\pi i \mu_1 q_\alpha}{k_B T \varepsilon_0 k}\right)\frac{\sin[k\sigma_{\text{IL}}(1+R)/2]}{k\sigma_{\text{IL}}(1+R)/2}, \quad (5)$$

where μ_1 is the dipole-moment of the dipolar solute, q_α the charge of αth type ion, ε_0 the static dielectric constant and r_c the distance of the closest approach between the solute dipole and the ionic species. R denotes the solute-IL size-ratio, $\frac{\sigma_{\text{solute}}}{\sigma_{\text{IL}}}$, σ_{IL} being the effective diameter of an IL determined from the ionic sizes. $S^{\text{ion}}_{\alpha\beta}(k,t)$, the isotropic ion dynamic structure factor, has been obtained from known results [22,23] (Supporting information).

Subsequently, the normalized solvation energy–energy correlation function due to the dipole–dipole interaction is given by

$$S_{sd}(t) = \frac{C_{sd}(t)}{C_{sd}(t=0)}, \quad (6)$$

and that due to dipole–ion interaction

$$S_{si}(t) = \frac{C_{si}(t)}{C_{si}(t=0)}. \quad (7)$$

The individual response functions given by Eqs. (6) and (7) constitute the solvation response function measured in experiments. The total solvation response function (S_{ss}) and the average solvation time ($\langle\tau_{ss}\rangle$) are calculated as follows: $S_{ss}(t) = (1-f)S_{sd}(t) + fS_{si}(t)$ and $\langle\tau_{ss}\rangle = \int_0^\infty dt S_{ss}(t)$. Based on experimental observations in electrolyte solutions [24] and earlier success of the present theory for several ILs [7,8], we have set $f = 0.2$, although a small variation does not alter the qualitative feature of the predicted results. Furthermore, the dipole–dipole and ion–dipole interaction contributions to dynamic Stokes' shift have been

calculated [7,8,11,12] respectively from Eqs. (3) and (4) at $t = 0$. Other necessary parameters are provided in Tables S2 and S3 (Supporting information).

3. Numerical results and discussion

The calculated dynamic Stokes' shifts summarized in Table 1 indicates that the total shifts predicted for C153 in these ILs are much larger than those obtained with the same probe in more common imidazolium and phosphonium ILs [7,8]. These shift values have been obtained by using the effective dipole moment (μ_{eff}^{Cavell}) [10] determined via Cavell's equation where the magnitude (ΔS) of the slowest dielectric dispersion is used as input. Strikingly, the dipolar interaction between the solute and dipolar imidazolium cation is found to contribute ~75–85% of the total predicted shift ($\Delta\nu_{tot}^{t}$) for each of these $[Al(hfip)_4]^-$ containing ILs. The scenario remains the same even if the shift values are calculated (shown in parenthesis) by using the effective dipole moment (μ_{eff}^{MSA}) from ε_0 via the MSA [9]. This is in sharp contrast to the normal belief that Stokes' shift in ILs should be dominated by the dipole–ion ($1/r^2$) interaction between the solute and the constituent ions of the ILs. In addition, this domination of dipole–dipole ($1/r^3$) interaction contribution is different from the calculations [7,8] for the same solute in imidazolium ILs with anions other than $[Al(hfip)_4]^-$ where ~40–50% dipolar contribution ($\Delta\nu_{sd}^{t}$) to the total shift was predicted. Eventhough a role for solute–cation dipolar interaction in determining the shift in ILs was hinted at in earlier reports [25,26], such an overwhelming contribution from the solute-IL dipolar interaction was never anticipated before. A closer inspection of Table 1 also indicates while the ion–dipole interaction contribution ($\Delta\nu_{si}^{t}$) increase as ε_0 decreases, $\Delta\nu_{sd}^{t}$ attains the largest value for that IL in which the combined effects of ε_0 and σ_+ (see Table S2) becomes the maximum. Effects of ion-size on $\Delta\nu_{sd}^{t}$ and $\Delta\nu_{si}^{t}$ are best illustrated as follows. $\Delta\nu_{sd}^{t}$ for [allyl-mim]$^+$ $[Al(hfip)_4]^-$ is larger than that for [C6-mim]$^+$ $[Al(hfip)_4]^-$ because of smaller σ_+ for the former (6.84 Å) than the latter (7.76 Å) although ε_0 values are quite similar for these ILs (see Table S1). Again, $\Delta\nu_{si}^{t}$ for [C2-mim]$^+$ $[Al(hfip)_4]^-$ is nearly half of that calculated for [bmim]$^+$ $[BF_4]^-$ because $[Al(hfip)_4]^-$ is ~2.5 times larger in size than that of $[BF_4]^-$ eventhough σ_+ for [C2-mim]$^+$ and [bmim]$^+$ are similar and ε_0 values of these ILs comparable at comparable temperatures[3,14] (but not the densities[8]). The difference in $\Delta\nu_{sd}^{t}$ values between these two ILs can be attributed largely to the difference in corresponding liquid densities [27].

The ion-size effect on dynamic Stokes shift is further explored in Figure 1 where shift values measured and calculated for C153 in other ILs along with the calculated total shifts ($\Delta\nu_{total}^{t}$) for these ILs are shown as a function of size-ratio, $P = \sigma_+/\sigma_-$. Figure 1 indicates a substantial correlation between $\Delta\nu_{total}^{t}$ and R' ~0.7, and the predicted monotonic decrease of $\Delta\nu_{total}^{t}$ with P arises from the reduced solute–ion interactions at increased P. Note the degree of correlation does not significantly alter upon non-inclusion (broken lines, R' ~0.6) or inclusion (solid line, R' ~0.7) of the calculated shift values for these aluminate ILs in the fit. The fact that the calculated shifts for these ILs follow the same linear correlation with P as observed for other ILs suggests that these predictions are qualitatively correct and should therefore be reexamined in experiments. Since $\mu_{eff}^{Cavell} > \mu_{eff}^{MSA}$ for these liquids (see Table S3), the predicted shifts are larger when μ_{eff}^{Cavell} is used in calculations. However, this was not the case for other ionic liquids as $\mu_{eff}^{Cavell} \approx \mu_{eff}^{MSA}$ for them (Table S3).

Calculated decays of the solvation response function, $S_{ss}(t)$, are shown in Figure 2 for two representative ILs, [C2-mim]$^+$ $[Al(hfip)_4]^-$ and [C6-mim]$^+$ $[Al(hfip)_4]^-$ as several properties of them, for example, cation-size (σ_+), dielectric relaxation time constant (τ) and the associated stretching exponent (α) are widely different. Figure 2 clearly indicates that the decays are bimodal, which is the case for the other aluminate ILs also. As observed earlier [7,8,32], the bimodal decays have been found to consist of a fast exponential and a slow stretched exponential components. When a libration band centered around 100 cm^{-1} is assigned to carry out the remaining dispersion [28–31], $[(\varepsilon_0 - S) - n^2]$ (n^2 being the square of the refractive index and fixed at 2) and incorporated in calculations, the bimodal decays become only

Table 1
Calculated dynamic Stokes' shifts for C153 in aluminate ILs at 343 K.[a]

Ionic liquid	Dipole–dipole contribution, $\Delta\nu_{sd}^{t}$(cm^{-1})	Ion–dipole contribution, $\Delta\nu_{si}^{t}$ (cm^{-1})	Total[c] $\Delta\nu_{total}^{t}$ (cm^{-1})	% of total Stokes' shift from dipole–dipole interaction
[allyl-mim]$^+$ $[Al(hfip)_4]^-$	2894 (2162)[b]	495	3389 (2657)	85 (81)
[C4-mim]$^+$ $[Al(hfip)_4]^-$	2014 (1650)	577	2691 (2227)	77 (74)
[C2-mim]$^+$ $[Al(hfip)_4]^-$	2151 (1888)	686	2837 (2574)	76 (73)
[C6-mim]$^+$ $[Al(hfip)_4]^-$	1860 (1457)	452	2312 (1909)	80 (76)
[C2-mmim]$^+$ $[Al(hfip)_4]^-$	3231 (2143)	469	3700 (2612)	87 (82)
[C4-mmim]$^+$ $[Al(hfip)_4]^-$	2804 (1829)	433	3237 (2262)	87 (81)

[a] Shift calculated using effective dipole moment (μ_{eff}^{Cavell}) obtained from Cavell's equation.
[b] Values in parenthesis calculated by using the effective dipole moment (μ_{eff}^{MSA}) from the MSA. μ_{eff}^{Cavell} and μ_{eff}^{MSA} for these ILs are summarized in Table S3 (Supporting information).
[c] $\Delta\nu_{total}^{t} = \Delta\nu_{sd}^{t} + \Delta\nu_{si}^{t}$.

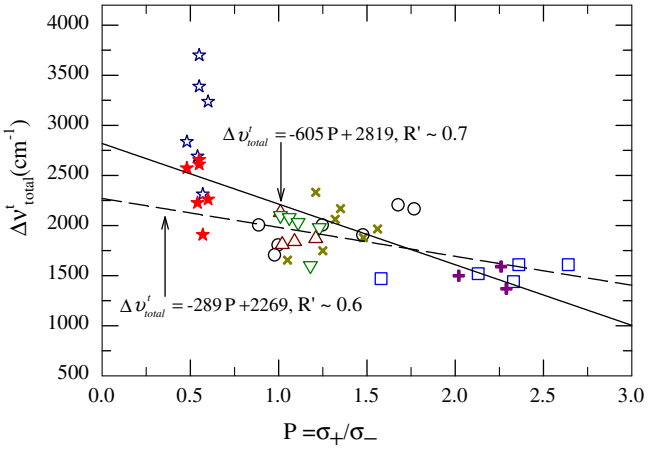

Figure 1. Correlation between the total dynamic Stokes' shift and the ratio between the ion diameters, $P = \sigma_+/\sigma_-$ for C153 in various ILs. Black circles, dark red triangles, dark green inverted triangles, and blue squares denote measured shifts for imidazolium, pyrrolidinium, ammonium and phosphonium ILs respectively. Dark yellow crosses and dark pink pluses denote respectively the calculated shifts for imidazolium, and phosphonium ILs. Dark blue stars denote the predicted shifts for the aluminate ILs considered where effective dipole-moment values used are those obtained from Cavell's equation. Red filled stars are predicted shifts obtained using dipole moment from the MSA. Note while the dashed lines describes a correlation without including the predicted shifts for the aluminate ILs, the solid line is obtained after including both sets of the predicted shifts for these ILs. R' denotes correlation coefficient. References from which shift data taken are provided in Table S4 (Supporting information). (For interpretation of the references to color in this figure legend, the reader is referred to the web version of this article.)

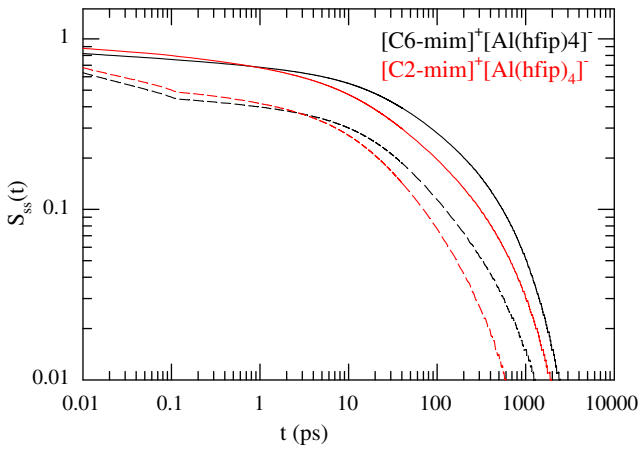

Figure 2. Effects of librational band (~100 cm^{-1}) on calculated normalized solvation response functions for C153 in two representative aluminate ionic liquids, $[C6\text{-}mim]^+$ $[Al(hfp)_4]^-$ (black lines) and $[C2\text{-}mim]^+$ $[Al(hfp)_4]^-$ (red lines) at 343 K. While the solid lines represent calculations without considering the libration contribution, the dashed lines the calculations after incorporating the libration mode. Eq. (5) of Ref. [17] has been used to incorporate the libration contribution. (For interpretation of the references to color in this figure legend, the reader is referred to the web version of this article.)

faster (broken lines) keeping the qualitative features intact. This was also observed previously for solvation dynamics of C153 in liquid amides [33,34]. Parameters obtained from fitting the solvation response functions calculated for these aluminate ILs in the absence and presence of the libration band are summarized in Table 2. Table 2 indicates that the initial fast component of all the predicted decays is characterized by a time-constant (τ_1) $\leqslant$ 20 fs even after using the available DR data [3] measured with 'limited' frequency coverage. Interestingly, the amplitude of the ultrafast component (a_1) increases up to ~50% of the total decay with time-constant as fast as ~5 fs when one includes the libration contribution in the solvation energy relaxation. Note such a fast component was not observed in experiments [32] or simulations [35–40] with ILs at room temperature but a simulation study of $[Im_{11}]^+$ $[Cl]^-$ at elevated temperature (425 K) [41] reported a large fast component (~75%) with a time-constant of ~70 fs. The slow time-constant (τ_2), which also does not change appreciably upon inclusion of the libration contribution, appears very similar to the predictions for other imidazolium ILs at ~338 K [8]. Similarities in the amplitude of the slow component (a_2) and the solvation stretching exponent (β) coupled with the closeness in τ_2 then make the calculated average solvation times ($\langle\tau_{ss}\rangle$) for these aluminate ILs comparable to those predicted for other imidazolium ILs with similar viscosities at elevated temperature [8].

The predictions that a_1 becomes as large as 50% and $\langle\tau_{ss}\rangle$ reduces by a factor of ~4–9 upon inclusion of libration originate from assigning whole of the undetected [3] high frequency dispersion ($[(\varepsilon_0 - S) - n^2]$) to the libration band because this dispersion magnitude critically determines the amplitude of the ultrafast polar solvation response [33]. This strongly suggests the importance of the high frequency coverage and accurate description of the dielectric relaxation data for a better performance of the present theory, which is further demonstrated in Figure 3 where decays of $S_{sd}(t)$ with and without libration contribution, and $S_{si}(t)$ are shown for $[C2\text{-}mim]^+$ $[Al(hfip)_4]^-$. Figure 3 suggests that the decay of $S_{sd}(t)$, which in the absence of libration is slower than that of $S_{si}(t)$ at long time ($t > 30$ ps), becomes faster after inclusion of libration contribution. The interesting point here is that because center-of-mass diffusion of the particles govern the decay of $S_{si}(t)$ as opposed to the much faster orientational readjustment of dipolar species for $S_{sd}(t)$, the decay of $S_{si}(t)$ is expected to be slower than that of $S_{sd}(t)$. Our best fits to $S_{si}(t)$ (bi-exponential) and $S_{sd}(t)$ (fast exponential followed by a slow stretched one) have produced comparable τ_2 (~50 and ~40 ps, respectively) but a β value of 0.32 makes the decay of $S_{sd}(t)$ in the absence of libration slower than that of $S_{si}(t)$. Subsequent inclusion of libration considerably reduces τ_2 (17 ps) for $S_{sd}(t)$ but β remains unchanged and consequently $S_{sd}(t)$ decays at a rate faster than the previous case. The same is observed for other ILs considered here as well, stressing the need for a complete DR measurements with wider frequency coverage to better understand the dynamic solvation response in these newly synthesised ILs.

We next investigate to what extent the dynamic continnum model by Rips, Klafter and Jortner (RKJ) [42] is valid in predicting the dynamics in these ILs and explore the origin of the calculated sub-50 fs solvation response. The RKJ theory is one of the simplest theories that directly connects the polar solvation response to the measured DR data but neglects completely the solute–solvent and solvent–solvent static structural correlations. We therefore compare in Figure 4 the decay of $S_{sd}(t)$, calculated without libration contribution, in the long wavelength ($k \to 0$) limit for $[C2\text{-}mim]^+$ $[Al(hfip)_4]^-$ with the corresponding RKJ predictions. A good agreement between $S_{sd}(t, k \to 0)$ and RKJ predictions indicates a simple theory like the RKJ can qualitatively predict the dipolar part of the solvation response in these ILs as it did earlier for common polar solvents [43]. However, the RKJ theory predicts a slower decay than that of $S_{sd}(t, k \to 0)$ at later times because of the neglect of the static solvent structural correlations in the long wavelength limit. In this time regime, $S_{sd}(t)$ decays faster because of participation of both the solute and solvent translational modes [18–21]. The dramatic break-down for the RKJ theory occurs because of its inability to account for the much slower diffusive relaxation of the ion–dipole interaction component, $S_{si}(t)$, in ILs.

Table 2
Parameters obtained from fitting the calculated solvation response functions for C153 in aluminate ILs at 343 K with and without the libration contribution[a].

Ionic liquid		a_1	τ_1 (fs)	a_2	τ_2 (ps)	β	$\langle\tau_{ss}\rangle$(ps)
$[allyl\text{-}mim]^+$ $[Al(hfip)_4]^-$	Without libration	0.04	5	0.96	38.0	0.44	95.0
	With libration	0.39	5	0.61	33.7	0.49	20.6
$[C4\text{-}mim]^+$ $[Al(hfip)_4]^-$	Without libration	0.18	9	0.82	48.0	0.41	121.0
	With libration	0.52	6	0.48	30.5	0.51	14.7
$[C2\text{-}mim]^+$ $[Al(hfip)_4]^-$	Without libration	0.11	10	0.89	32.0	0.38	108.0
	With libration	0.48	6	0.52	23.8	0.49	12.4
$[C6\text{-}mim]^+$ $[Al(hfip)_4]^-$	Without libration	0.21	8	0.79	94.0	0.45	181.0
	With libration	0.54	6	0.46	50.8	0.52	23.4
$[C2\text{-}mmim]^+$ $[Al(hfip)_4]^-$	Without libration	0.17	20	0.83	28.0	0.38	89.0
	With libration	0.35	6	0.65	29.5	0.44	19.2
$[C4\text{-}mmim]^+$ $[Al(hfip)_4]^-$	Without libration	0.28	10	0.72	46.0	0.42	96.0
	With libration	0.41	6	0.59	44.7	0.46	26.4

[a] DR data and other parameters necessary for the above calculations are summarized in Tables S1 & S2 (Supporting information).

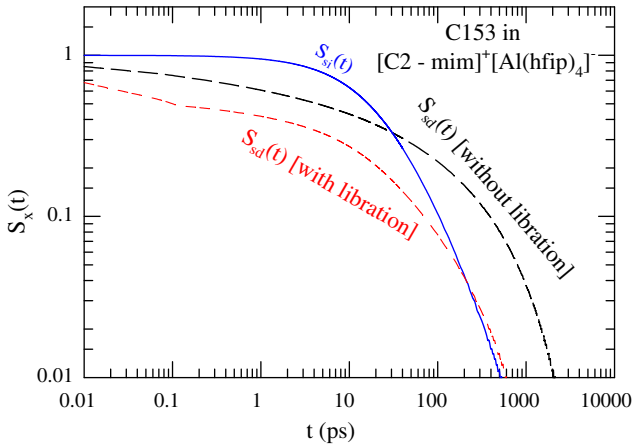

Figure 3. Individual interaction components, $S_{sd}(t)$ and $S_{si}(t)$, of the solvation response functions and importance of high frequency coverage for DR measurements in aluminate ILs. The dipole–dipole interaction component $S_{sd}(t)$ is shown by the broken lines and the ion–dipole component by the solid line. While the red lines denote calculations with the libration mode and black lines without the libration mode. (For interpretation of the references to color in this figure legend, the reader is referred to the web version of this article.)

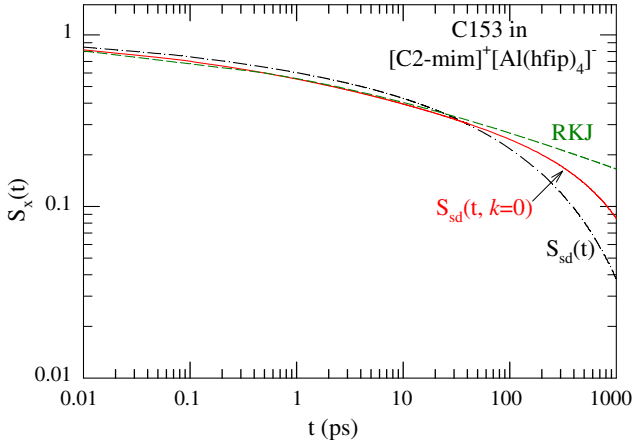

Figure 4. Performance of a dynamic continuum model (RKJ theory here) and the domination of the orientational relaxation in producing the ultrafast component. Tagged symbols denote predictions from the RKJ model and the present theory.

The decay of $S_{sd}(t, k \to 0)$ calculated for [C2-mim]$^+$ [Al(hfip)$_4$]$^-$ in the absence of libration contribution, upon fitting, produces a fast time-constant of ~10 fs ($a_1 \sim 30\%$) and a slow time constant of ~60 ps with $\beta \approx 0.3$. The IL, [C2-mim]$^+$ [Al(hfip)$_4$]$^-$, here serves as a representative example as qualitatively similar results have been obtained for other aluminate ILs as well. This observation clearly indicates that the sub-50 fs response in $S_{ss}(t)$ arises solely from the collective orientational response of the dipolar ions in these ILs. Note our earlier calculations for room temperature imidazolium ILs [17] has already shown that, like in common polar solvents, the ultrafast response in dipolar ILs originates also from the collective orientational relaxation. This argument is further supported by recent simulations of ILs [44,45] and molten NaCl [46] which find no evidence for translational contributions in $\varepsilon(z)$ obtained at the microwave regime (300 MHz–300 GHz). With such a current understanding of the microwave dielectric relaxation data, the dominating role for the collective orientational polarization relaxation in producing the ultrafast solvation response in dipolar ILs becomes even more evident.

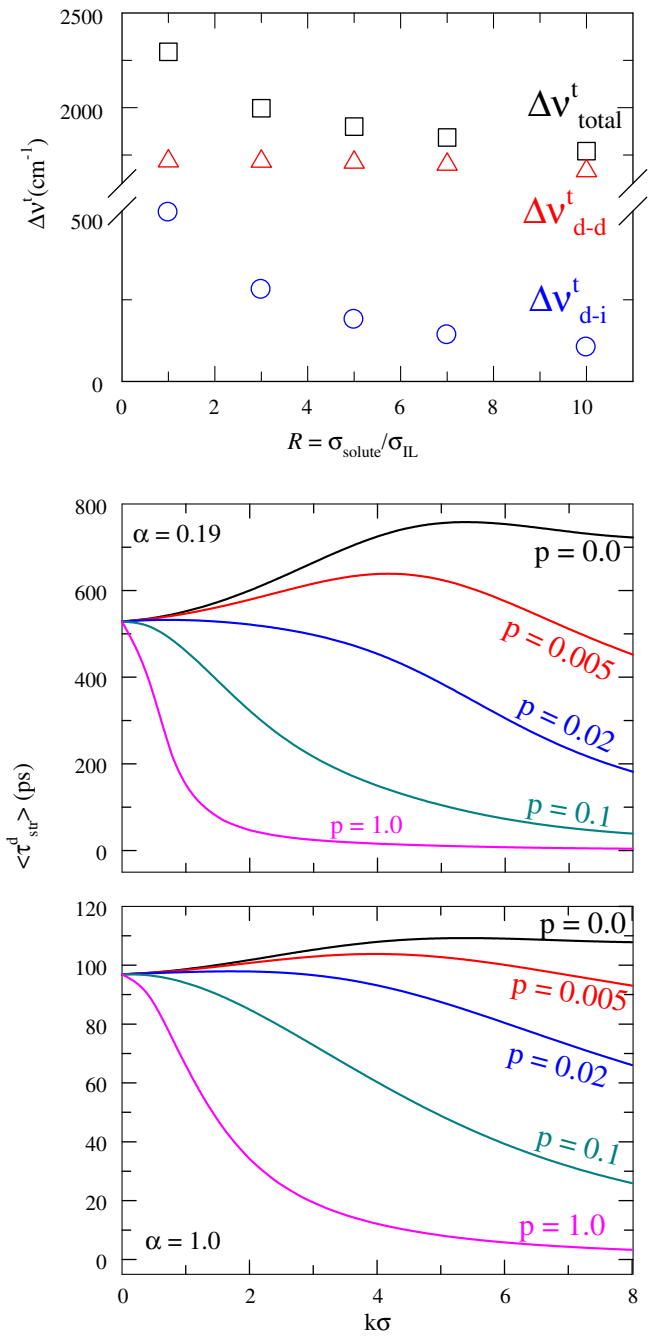

Figure 5. Solute size dependence of dynamic Stokes shift (upper panel) and relative importance of solvent rotational and translational modes for solvation energy relaxation in ILs (middle and lower panels). Various interaction contributions to the calculated total shift (squares) are labeled as follows: triangles denote the solute-IL size ratio (R) dependence of dipole–dipole interaction contribution, and circles the ion–dipole contribution. Note the size of an IL molecule has been kept fixed. The calculations are for C153 in [C4-mim]$^+$ [Al(hfip)$_4$]$^-$ at 343 K. The role of solvent translation is quantified for both heterogeneous (middle panel) and homogeneous liquids (lower panel). Note the results shown in the lower panel have been obtained with the same dielectric relaxation data as used for results in the middle panel but with $\alpha = 1.0$.

We now present in the upper panel of Figure 5 the results of our model calculations on solute-IL size-ratio dependence of interaction contributions to the total shift for C153 in [C4-mim]$^+$ [Al(hfip)$_4$]$^-$. Calculated total shift decreases, as evidenced in the upper panel, with the increase in size ratio ($R = \sigma_{solute}/\sigma_{IL}$), the total decrease for changing R from 1 to 10 being only ~25%. This is because of the dominance of the dipole–dipole interaction

contribution which reduces only by ~3% in this range of size-ratio variation. In contrast, the ion–solute ion–dipole interaction contribution reduces by ~80%. Such a strong size-effect on ion–dipole contribution arises from the inverse dependence of $c^{10}_{sz}(k)$ on $(1+R)$ (see Eq. (5)). The dependence of dipolar contribution is weaker because size-effect in dipole–dipole direct correlation function enters only via the solute number density [9] which is present at infinite dilution. In the limit of extremely large solute ($R = 50$) where solute packing fraction becomes substantial, however, the dipolar contribution becomes nearly one-fifth of that at $R = 1$, and the ion–dipole contribution vanishingly small. Note data in Table S5 (Supporting information) reveals measured shifts in normal solvents of comparable polarity (ε_0) are less than those in ILs. Moreover, the measured shifts in non-dipolar ILs are smaller than those in dipolar counter-parts. These observations probably constitute an indirect experimental evidence in favor of the relative importance of solute-IL dipole–ion and dipole–dipole interaction contributions to the total shift.

The relative importance of translational and rotational modes in the decay of dipolar interaction contribution is shown in the last two panels of Figure 5 where average relaxation time obtained for different values of $(p = D_T/D_R\sigma^2_{IL})$ from the decay of the normalized dipolar dynamic structure factor, $S^{10}_{solvent}(k,t)$, are shown as a function of wave-vector. As observed for dipolar liquids [47], participation of the translational modes shortens the relaxation time ($\langle\tau^d_{str}\rangle$) considerably, the wavevector dependence of $\langle\tau^d_{str}\rangle$ being more pronounced for inhomogeneous liquid (middle panel, $\alpha = 0.19$) than that for homogeneous one (lower panel, $\alpha = 1.0$) (see also Figure S6, Supporting information). Interestingly however, the rotation dominates the over-all relaxation because too much efficiency of translation at large wavevectors makes the latter insignificant.

4. Conclusion

The present work shows that there could be dipolar ILs such as the present ones where the solvation energy for an excited dipolar solute molecule might be dominated by the solute-IL dipolar interaction rather than the anticipated solute-IL dipole-ion interaction. A weak solute-size dependence is predicted to arise from the domination of the dipole–dipole interaction contribution to the total shift. More importantly, the ultrafast response in dipolar ILs has been found to originate from the collective orientational response of the ILs. A number of new results have been predicted for these fascinating ILs which should be experimentally verified. Once done, the proposed measurements are likely to provide resolutions to the ongoing debate over the interpretation of Stokes' shift dynamics [48,49] in these completely new class of solvents.

Acknowledgment

SD thanks the CSIR, India for a research fellowship. RB acknowledges the encouragement received from Profs. B. Bagchi and M. Maroncelli.

Appendix A. Supplementary data

Supplementary data associated with this article can be found, in the online version, at doi:10.1016/j.cplett.2011.05.027.

References

[1] S. Bulut et al., Chem. Eur. J. 16 (2010) 13139.
[2] H. Jin et al., J. Phys. Chem. B 112 (2008) 81.
[3] M.-M. Huang, S. Bulut, I. Crossing, H. Weingartner, J. Chem. Phys. 133 (2010) 101101.
[4] M. Ediger, Annu. Rev. Phys. Chem. 51 (2000) 99.
[5] A. Triolo, O. Russina, H.-J. Bleif, Di Cola, J. Phys. Chem. B. 111 (2007) 4641.
[6] J.N.A. Canongia Lopes, A.A.H. Padua, J. Phys. Chem. B. 110 (2006) 3330.
[7] H.K. Kashyap, R. Biswas, J. Phys. Chem. B. 114 (2010) 254.
[8] H.K. Kashyap, R. Biswas, J. Phys. Chem. B. 114 (2010) 16811.
[9] C.G. Gray, K.E. Gubbins, Theory of Molecular Fluids, Vol. I, Clarendon, Oxford, 1984.
[10] E.A.S. Cavell, P.C. Knight, M.A. Sheikh, J. Chem. Soc. Faraday Trans. 67 (1971) 2225.
[11] B. Guchhait, H.A.R. Gazi, H.K. Kashyap, R. Biswas, J. Phys. Chem. B 114 (2010) 5066.
[12] H.A.R. Gazi, B. Guchhait, S. Daschakraborty, R. Biswas, Chem. Phys. Lett. 501 (2011) 358.
[13] A. Stoppa, J. Hunger, R. Buchner, G. Hefter, A. Thoman, H. Helm, J. Phys. Chem. B 112 (2008) 4854.
[14] J. Hunger, A. Stoppa, S. Schrodle, G. Hefter, R. Buchner, Chem. Phys. Chem. 10 (2009) 723.
[15] I. Crossing, I. Raabe, Angew. Chem. Int. Ed. 43 (2004) 2066.
[16] H.V. Spohr, G.N. Patey, J. Chem. Phys. 129 (2008) 064517.
[17] H.K. Kashyap, R. Biswas, J. Phys. Chem. B 112 (2008) 12431.
[18] H.K. Kashyap, R. Biswas, Ind. J. Chem. 49A (2010) 685.
[19] B. Bagchi, Annu. Rev. Phys. Chem. 40 (1989) 115.
[20] B. Bagchi, R. Biswas, Adv. Chem. Phys. 109 (1999) 207.
[21] B. Bagchi, A. Chandra, Adv. Chem. Phys. 80 (1991) 1.
[22] P. Attard, Phys. Rev. E. 48 (1993) 3604.
[23] A. Chandra, B. Bagchi, J. Chem. Phys. 110 (1999) 10024.
[24] C.F. Chapman, M. Maroncelli, J. Phys. Chem. 95 (1991) 9095.
[25] E.W. Castner Jr., J.F. Wishart, H. Shirota, Acc. Chem. Res. 40 (2007) 1217.
[26] S. Arzhantsev, N. Ito, M. Heitz, M. Maroncelli, Chem. Phys. Lett. 381 (2003) 278.
[27] S. Daschakraborty, R. Biswas, J. Phys. Chem. B. 115 (2011) 4011.
[28] D.A. Turton et al., J. Am. Chem. Soc. 131 (2009) 11140.
[29] G. Giraud, C.M. Gordon, I.R. Dunkin, K. Wynne, J. Chem. Phys. 119 (2003) 464.
[30] H. Shirota, E.W. Castner Jr., J. Phys. Chem. B 109 (2005) 21576.
[31] B.-R. Hyun, S.V. Dzyuba, R.A. Bartsch, E.L. Quitevis, J. Phys. Chem. A 106 (2002) 7579.
[32] S. Arzhantsev, H. Jin, G.A. Baker, M. Maroncelli, J. Phys. Chem. B 111 (2007) 4978.
[33] R. Biswas, B. Bagchi, J. Phys. Chem. 100 (1996) 1238.
[34] H.K. Kashyap, R. Biswas, J. Chem. Phys. 125 (2006) 174506.
[35] Y. Shim, J. Duan, M.Y. Choi, H.J. Kim, J. Chem. Phys. 119 (2003) 6411.
[36] Y. Shim, J. Duan, M.Y. Choi, H.J. Kim, J. Chem. Phys. 122 (2005) 044511.
[37] M.N. Kobrak, V. Znamenskiy, Chem. Phys. Lett. 395 (2004) 127.
[38] M.N. Kobrak, J. Chem. Phys. 123 (2006) 064502.
[39] C.J. Margulis, Mol. Phys. 102 (2004) 829.
[40] Z. Hu, C.J. Margulis, J. Phys. Chem. B 110 (2006) 11025.
[41] B.L. Bhargava, S. Balasubramanian, J. Chem. Phys. 123 (2005) 144505.
[42] I. Rips, J. Klafter, J. Jortner, J. Chem. Phys. 88 (1988) 3246.
[43] M.L. Horng, J.A. Gardecki, A. Papazyan, M. Maroncelli, J. Phys. Chem. 99 (1995) 17311.
[44] C. Schroder, C. Wakai, H. Weingartner, O. Steinhauser, J. Chem. Phys. 126 (2007) 084511.
[45] C. Schroder, M. Haberler, O. Steinhauser, J. Chem. Phys. 131 (2009) 114504.
[46] X. Song, J. Chem. Phys. 131 (2009) 044503.
[47] A. Chandra, B. Bagchi, J. Chem. Phys. 91 (1989) 1829.
[48] A. Samanta, J. Phys. Chem. Lett. 1 (2010) 1557.
[49] A. Samanta, J. Phys. Chem. B 110 (2006) 13704.